Nanostructured electrodes based on multiwalled carbon nanotube/glyconanoparticles for the oriented immobilization of bilirubin oxidase: Application to the electrocatalytic O2 reduction

Marie Carrière, Paulo Henrique M. Buzzetti, Karine Gorgy, Fabien Giroud, Hong Li, Redouane Borsali, Serge Cosnier

Nanostructured electrodes based on multiwalled carbon nanotube/glyconanoparticles for the oriented immobilization of bilirubin oxidase: Application to the electrocatalytic O_2 reduction

Marie Carrière [a,b,‡], Paulo Henrique M. Buzzetti [a,‡], Karine Gorgy [a], Fabien Giroud [a], Hong Li [b], Redouane Borsali [b] and Serge Cosnier [a,*]

[a] Univ Grenoble Alpes, DCM UMR 5250, F-38000 Grenoble, France. CNRS, DCM UMR 5250, F-38000 Grenoble, France
[b] Univ Grenoble Alpes, CNRS, CERMAV, F-38000 Grenoble, France
‡ These authors contributed equally
* serge.cosnier@univ-grenoble-alpes.fr

Here we describe the design and the characterization of novel electrode materials consisting of multi-walled carbon nanotubes coated with glyconanoparticles (GNPs) functionalized with anthraquinone sulfonate. The resulting modified electrodes were characterized by scanning electron microscopy and cyclic voltammetry. Their electrochemical behavior reveals a stable pH-dependent redox signal characteristic of anthraquinone sulfonate. Immobilization of bilirubin oxidase on these three-dimensional electrodes leads to the electroenzymatic reduction of O_2 to water with an onset potential of 0.5 V/SCE (saturated calomel electrode). A catalytic cathodic current of 174 µA (0.88 mA cm^{-2}) at 0.1 V/SCE, demonstrates that glyconanoparticles modified by anthraquinone sulfonate were able to interact and orientate bilirubin oxidase by electrostatic interactions.

Keywords: nanomaterial design; MWCNTs-based electrode; glyconanoparticles, host-guest interaction, oxygen electroreduction.

1. Introduction

Among the multicopper oxidases for which direct electron transfer (DET) between redox centers of enzymes and electrodes has been observed, bilirubin oxidases have been widely used in recent years in different bioelectrochemical applications such as the design of bilirubin sensors and biofuel cells [1]. In particular, bilirubin oxidase from *Myrothecium verrucaria* (MvBOD) is well known for its high stability, high activity at neutral pH for O_2 reduction and for its commercial availability [2]. MvBOD contains four copper ions classified into Type 1 (T1) Cu site close to the protein envelope (from 5 to 8 Å) [3] and a Type 2–3 (T2/3) Cu cluster. It is well admitted that the first step of the O_2 reduction is the transfer of electrons (from substrates or electrodes) to the mononuclear site (T1), followed by the transfer to the trinuclear site (T2/T3) where the four-electron four-proton dioxygen reduction into water takes place [4]. Electron transfer between MvBOD and an electrode can be achieved by mediated electron transfer (MET) using either a redox mediator as an electron shuttle or by DET between the enzyme active site and the electrode surface [5–10]. Regarding MET, various redox mediators have already been successfully used such as 2,2′-azino-bis(3-ethylbenzothiazoline-6-sulfonic acid) diammonium [11], metal complexes [12,13], redox polymers [14] and more recently glyconanoparticles modified with redox compounds [15,16].

However, the use of redox mediators can be confronted with their potential toxicity in solution or even with a low stability and their immobilization can prove to be difficult. Furthermore, redox mediators generally induce a minimum overvoltage necessary to achieve the maximum rate of enzyme-mediator electron transfer. In contrast, the DET reaction by definition occurs in the absence of any mediator and therefore offers a simpler setup. In addition, electron transfer can take place at a potential close to the natural standard redox potential of MvBOD. Nevertheless, to ensure a high DET rate, the ideal is obviously to shorten the distance between the T1 redox site of the enzyme and the electrode surface. Besides complex enzyme downsizing methods like deglycosylation [17], many research efforts have been conducted to design electrode materials allowing a close proximity of the T1 site of MvBOD to a conductive surface via a controlled orientation of MvBOD.

Considering that the T1 site of MvBOD presents positively charged amino acid residues [3], the favorable positioning of MvBOD at the electrode surface was mainly achieved by electrostatic interactions combined with π-π interactions with negatively charged electrodes.

Electrodes modified with carboxylate and sulfonate groups have thus been used successfully to promote efficient DET [18]. In a similar vein, MvBOD cathodes were thus developed by modifying the surfaces of the electrodes with negatively charged compounds such as syringaldazine, bilirubin and its analogs [19–23].

In order to increase the surface density of enzyme connected to the electrode, three-dimensional electrodes such as single-walled carbon nanotube forest or multi-walled carbon nanotube compression were developed [9,24–26]. With the aim of designing new biodegradable or even biocompatible 3D nanostructures allowing a high density of spatially oriented enzyme, an elegant approach consists in immobilizing glyconanoparticles functionalized by orienting agents. Glyconanoparticles (GNPs) are obtained by self-assembly of polystyrene-block-β-cyclodextrin copolymer [27] and were already used in solution as a versatile redox platform to connect enzymes [15,16]. More recently, unmodified GNPs have also been immobilized on electrodes for the design of biosensors [28] or fluorescent materials [29].

Here, we describe the functionalization of GNPs by anthraquinone sulfonate via host-guest interactions and the immobilization of these redox GNPs onto an electrode coated with multiwalled carbon nanotubes. The resulting modified electrodes were used for the spatial orientation of MvBOD at the electrode and applied to the electroenzymatic reduction of O_2.

2. Results and discussion

2.1. Characterization of GNP_{PSCD} and GNP_{PSCD}/AQS

The self-assembly of the amphiphilic polystyrene-block-β-cyclodextrin copolymer by direct nanoprecipitation in water provides spherical GNPs consisting of a polystyrene core covered with a shell composed of cyclodextrin groups [15,16,28,29]. The morphology of GNPs in suspension in water used in this work (GNP_{PSCD}) were characterized by dynamic transmission electron microscopy. Fig. 1a shows that spherical nanoparticles were obtained with a relatively narrow size distribution, the average particle diameter being 20 nm. Thanks to the hydrophobic character of the cyclodextrin cavity, GNP_{PSCD} can be easily functionalized by host-guest interaction with hydrophobic compounds [15,30]. According to this principle, the GNP_{PSCD} has been modified by the inclusion of an aromatic anthraquinone sulfonate (AQS) thus creating a negatively charged shell. Compared to unmodified GNP_{PSCD}, stable functionalized nanoparticles (GNP_{PSCD}/AQS) showed no change in morphology or size distribution (Fig. 1b).

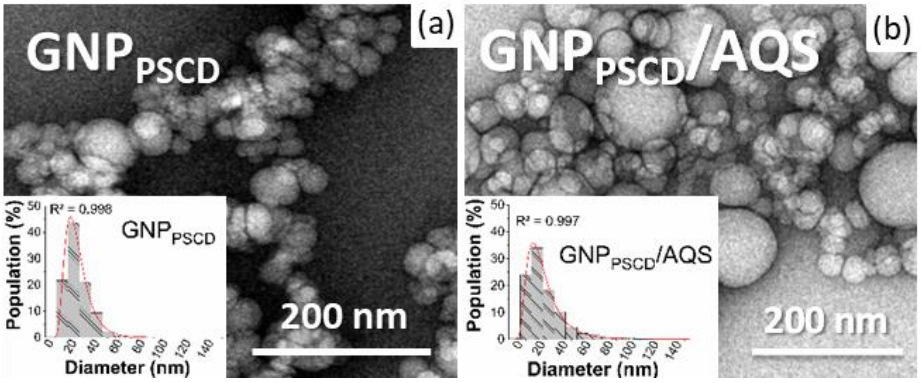

Fig. 1 TEM images showing (a) GNP_{PSCD} obtained by direct precipitation of polystyrene-block-β-cyclodextrin copolymer and (B) GNP_{PSCD} post-functionalized with AQS (GNP_{PSCD}/AQS). Inset: Its respective histogram showing the size distribution of the respective glyconanoparticles.

2.2. Electrochemical properties of MWCNT/GNP_{PSCD}/AQS

GNP_{PSCD}/AQS were deposited on carbon electrode previously modified with a multiwalled carbon nanotubes (MWCNTs) coating and the electrochemical properties of the resulting modified electrode was investigated by cyclic voltammetry in Britton-Robinson buffer at different pH values. At pH 2.5, Fig. 2a shows a well-defined reversible peak system at $E_{1/2}$ = – 0.24 V/SCE (ΔEp = 17 mV) that may be attributed to the two protons/two electrons reduction of anthraquinone groups. In accordance with Nernst's law, this redox couple was shifted to more negative values when the pH was increased. A linear potential/pH dependence (R^2 = 0.998, corresponding plot not shown) with a slope of - 56 mV per pH unit was observed corroborating the ratio of one proton to one electron. This phenomenon was already observed for the electrochemistry of GNP_{PSCD}/AQS glyconanoparticles in aqueous solution [30].

In addition, the current intensity of reductive peak varies linearly (R^2 = 0.997, corresponding plot not shown) with the scan rate, confirming the immobilization of GNP_{PSCD}/AQS onto MWCNT electrodes (Fig. 2b). The apparent surface coverage of AQS (Γ_{max} = 8.0 x 10^{-9} mol cm^{-2}), was estimated by integration of the charge under this peak system. Considering that the theoretical maximum surface coverage of a compact AQS layer is 1.1 - 1.7 x 10^{-10} mol cm^{-2} [31,32], the immobilization of GNP_{PSCD}/AQS equivalent to 48-72 compact monolayers of AQS clearly shows the interest of the three-dimensional structure. The stability of the adsorbed GNPs was investigated by continuous scanning the electrode potential through the AQS redox system (50 scans) in aqueous electrolyte. A negligible decrease of the current intensity of the anthraquinone redox system (12 %) was recorded, confirming the firm adsorption of the nanoparticles and the stable inclusion of AQS into the cyclodextrin cavity (Fig. 2c).

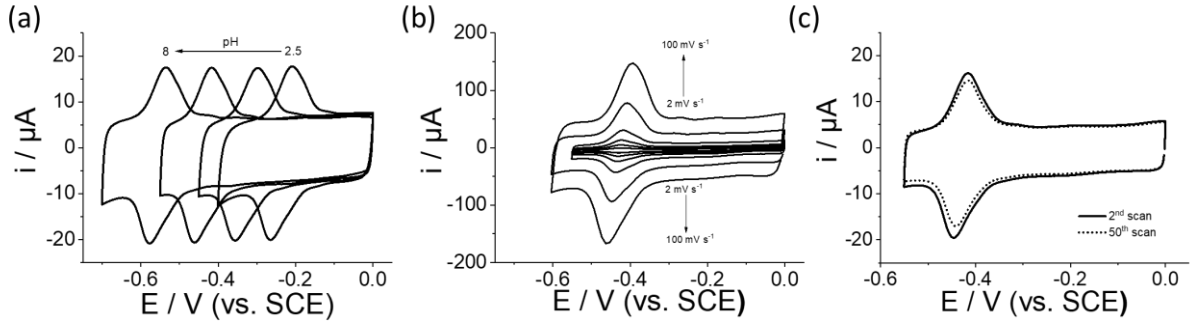

Fig. 2 Cyclic voltammetry recorded at glassy carbon electrode (3 mm diameter) covered with 20 µL of MWCNTs (5 mg mL^{-1} in NMP) and 50 µL of GNP_{PSCD}/AQS (a) in Britton-Robinson buffer at different pH 2.5, 4.0, 6.0 and 8.0 at 10 mV s^{-1} under Ar; (b) at different scan rates 2, 5, 10, 20, 50, and 100 mV s^{-1} in McIlvaine buffer at pH = 6.0 and (c) voltamperogram recorded after one cycle and 50 cycles at 10 mV s^{-1} in McIlvaine buffer at pH = 6.0.

To examine the configuration of GNP_{PSCD}/AQS after immobilization on the MWCNT electrode, SEM images were taken after depositing 50 µL of GNP_{PSCD}/AQS on the MWCNT electrode (Fig. 3a and 3b). A scratch was made on the modified electrode in order to observe the different layers successively deposited on the surface of the vitreous carbon electrode. Thus, the surface of the vitreous carbon electrode (1), a compact layer of MWCNTs (2) and a homogeneous deposit of nanoparticles (3) can be distinctly observed. Additionally, the inset of Fig. 3b shows well-defined nanospheres confirming the conservation of the GNP_{PSCD}/AQS morphology observed in solution after adsorption.

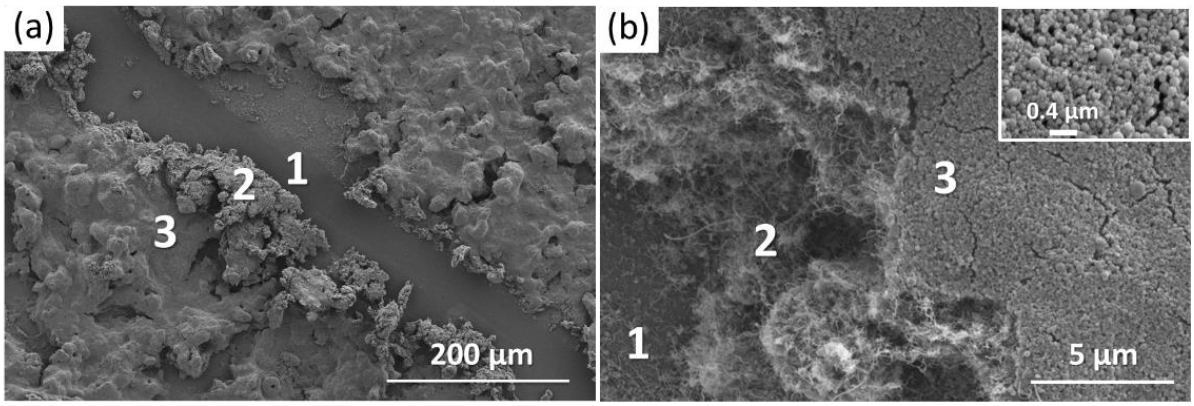

Fig. 3 (a) and (b) SEM images of GNP_{PSCD}/AQS deposited on MWCNTs at different magnifications. 3 layers are visible: the carbon electrode (1), the MWCNTs (2) and the GNP_{PSCD}/AQS (3).

2.3. Application to the electrical wiring of MvBOD

50 µL of MvBOD (5 mg mL^{-1}) were incubated on an MWCNT/GNP_{PSCD}/AQS electrode overnight and then the modified electrode was rinsed thoroughly for 10 minutes in a phosphate buffer solution pH = 7. The resulting bioelectrode was then characterized by cyclic voltammetry successively in an argon and dioxygen-saturated solution (Fig. 4a). While no faradaic current is observed under argon in the potential range from 0.1 to 0.5 V/SCE, a strong cathodic current appears from 0.5 V/SCE in the presence of dioxygen. The latter corresponds to the electro-enzymatic reduction of oxygen into water by the immobilized MvBOD via a DET process leading to a maximum current value of -174 µA at 0.1 V/SCE.

Control experiments were carried out by incubating the enzyme under the same conditions on electrodes modified by a deposit of MWCNTs or by a deposit of MWCNTs functionalized by unmodified GNP_{PSCD} (namely without AQS). Negligible catalytic current values of - 13 µA and - 8 µA were observed for MWCNT/MvBOD and MWCNT/GNP_{PSCD}/MvBOD configurations, respectively. With the aim to evaluate more precisely the influence of AQS on the catalytic reduction of O_2, the performance of a MWCNT electrode successively modified by AQS then MvBOD is examined. Compared to the same modified electrode without AQS, it appears that the catalytic current at 0.1 V/SCE (- 35 µA) is greater reflecting the efficient orientation of the enzyme generated by the sulfonate groups of AQS. These results clearly illustrate the beneficial role of AQS for the electrical connection of MvBOD whether in the presence or absence of GNPs. Additionally, the comparison with the MWCNT/GNP_{PSCD}/AQS/MvBOD configuration shows that although the onset potential seems identical, it appears that the catalytic current is 5 times lower than that obtained with the presence of adsorbed GNP_{PSCD}/AQS. This unambiguously demonstrates the interest of the three-dimensional structure of GNP_{PSCD}/AQS immobilized on MWCNT electrodes to obtain efficient DET from MvBOD.

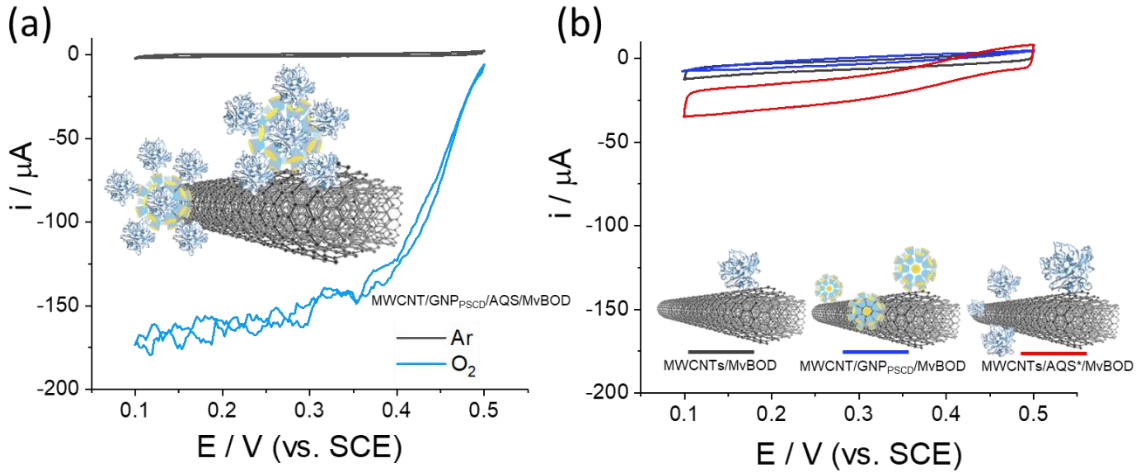

Fig. 4 Cyclic voltammetry recorded at 10 mV s^{-1} of (a) MWCNT/GNP_{PSCD}/AQS/MvBOD electrode in 0.2 mol L^{-1} phosphate buffer at pH = 7 under Ar and O_2 saturated solutions; (b) MWCNTs/MvBOD, MWCNTs/AQS/MvBOD and MWCNTs/GNP_{PSCD}/MvBOD electrodes in 0.2 mol L^{-1} phosphate buffer at pH = 7 under O_2 saturated solutions.

3. Conclusion

This work reports on the design and characterization of new original electrode material based on MWCNTs and glyconanoparticles modified by anthraquinone sulfonate as a negatively charged redox compound. It appears that the immobilization of the GNPs previously modified by AQS in solution, on the MWCNTs leads to a stable adsorption of the GNPs and does not affect the electroactivity and the spherical shape of the latter.

Importantly, these nanostructured electrodes have been successfully applied to the three-dimensional and spatially oriented immobilization of MvBOD for the efficient electroenzymatic reduction of O_2 paving the way for the design of novel biocathodes for bioelectrochemical applications.

4. Experimental section

4.1. Materials and reagents

All reagents (analytical grade) were purchased from Sigma-Aldrich. MvBOD (E.C.1.3.3.5 bilirubin oxidase from *Myrothecium verrucaria*, 10.8 U mg^{-1} solid) from Aldrich was used as received without further treatment. Multiwalled carbon nanotubes (MWCNTs) were obtained Sigma-Aldrich and used as received.

4.2. Material and methods

4.2.1. Electrochemistry measurements

Glassy carbon electrodes (diameter 3 mm) were obtained from ALS Co. (Japan) were polished with a 2 µm diamond paste purchased from Presi (France) and rinsed successively with acetone, ethanol, water and left to sonicate for 10 min in a mixture water/ethanol. The electrochemical characterizations were carried out in a three-electrode electrochemical cell using an Autolab potentiostat with Nova software version. A saturated calomel electrode (SCE) was used as reference electrode, while a wire of Pt was used as counter electrode. Stability and electrochemical tests were performed in 0.1 mol L^{-1} phosphate buffer, Britton-Robinson buffer or in McIlvaine buffer solutions at desired pH. Distilled water was passed through a Milli-Q water purification system (Millipore, 18 MΩ).

4.2.2. Preparation and characterization of glyconanoparticles (GNP_{PSCD})

GNP_{PSCD} were obtained as already described [30]. Specifically, an amount of 30 mg of copolymer synthetized as was already described was dissolved in 4 mL THF/H_2O solution (80: 20) w/w and stirred at 1000 rpm for 24 h. This resulting solution was added drop by drop using a syringe pump debit at 10.2 mL h^{-1} in 160 mL of Milli-Q water under stirring at 500 rpm. The solution was then stirred for 2 h at room temperature before THF removal under reduced pressure at 40 °C. The glyconanoparticles suspension obtained with a final concentration of 0.1875 mg L^{-1} was kept at 4 °C without further purification. For morphological glyconanoparticles characterization, TEM images were achieved.

4.2.3. Functionalization of GNP_{PSCD} with sodium anthraquinone-2-sulfonate (GNP_{PSCD}/AQS)

As already described [30], 3 mg of sodium anthraquinone-2-sulfonate (AQS) was added in 10 mL of GNP_{PSCD} suspension freshly prepared. After exposure of ultrasound for 2 h, the resulting solution was stirred for 12 h at room temperature and dialyzed to eliminate AQS excess for 72 h at room temperature (cut-off = 3.5 – 5 kDa, 72 h; 20 × 2 L of water, 300 rpm). The different GNP_{PSCD}/AQS suspensions were kept at 4 °C without further purification. These GNP_{PSCD}/AQS were characterized by TEM.

4.2.4. Preparation of the electrodes

- MWCNT/GNP_{PSCD}/AQS modified electrodes: MWCNT films were prepared from a 5.0 mg mL^{-1} suspension in NMP kept for 60 min under sonication. From this resulting black solution, 20 µL was deposited onto glassy carbon electrode (GCE). The organic solvent was removed under vacuum leading to the formation of a MWCNTs layer (step 1). The MWCNT electrodes were then incubated with 50 µL of a GNP_{PSCD}/AQS fresh solution. The electrodes were dried at room temperature and thoroughly rinsed with deionized water before CV characterization (step 2).
- MWCNT/GNP_{PSCD}/AQS/MvBOD modified electrodes: After steps 1 and 2, MWCNT/GNP_{PSCD}/AQS modified electrodes were incubated with 50 µL of MvBOD fresh solution (5 mg mL^{-1} in McIl pH 5.0, respectively) overnight at 4 °C (step 2). Before testing, electrodes were thoroughly rinsed with deionized water.
- MWCNT/GNP_{PSCD}/MvBOD modified electrodes: The same steps 1 and 2 were carried out in the same conditions but with unmodified GNP_{PSCD}.
- MWCNT/MvBOD modified electrodes: After step 1, electrodes were incubated with 50 µL of MvBOD fresh solution (5 mg mL^{-1} in McIl pH 5.0, respectively) overnight at 4 °C (step 2). Before testing, electrodes were thoroughly rinsed with deionized water.

- MWCNT/AQS/MvBOD modified electrodes: After step 1, electrodes were incubated with AQS (Γ = 5.25 x 10^{-9} mol cm^{-2}) in order to get the equivalent AQS recovery observed to of MWCNT/GNP_{PSCD}/AQS/MvBOD modified electrodes. The electrodes were thoroughly rinsed with deionized water and then were incubated with 50 µL of MvBOD fresh solution (5 mg mL^{-1} in McIl pH 5.0, respectively) overnight at 4 °C. Before testing, electrodes were thoroughly rinsed with deionized water

The surface coverage Γ of AQS was determined, where applicable, by integration of the charge recorded under the reduction peak of AQS by cyclic voltammetry at low scan rate by using the following equation $\Gamma = \frac{Q}{nFA}$, where Q is the integrated charge under the reduction signal of AQS, F is the Faraday constant, A is the geometric area of the electrode (A = 0.196 cm^2), and n is the number of electrons transferred (n = 2).

4.2.5. Scanning Electronic Microscopy (SEM) and Transmission Electron Microscopy (TEM) Images

SEM images of the different electrodes were carried out by FEI/Quanta FEG 250 scanning electron microscope (SEM, Hillsboro, OR, USA) with an accelerating voltage of 5 kV. The TEM images were registered with TEM-CAM 216 (TVIPS) camera at 200 kV using a JEOL 2100 Plus microscope equipped with a RIO16 (GATAN) camera.

Author Contributions

The manuscript was written through contributions of all authors. Conceptualization, M.C., P.H.M.B., K.G., F.G., R.B. and S.C.; formal analysis, M.C., P.H.M.B., K.G., F.G. and H.L.; investigation, M.C., P.H.M.B., K.G., F.G., H.L. and S.C.; data curation, M.C., P.H.M.B., K.G. and F.G.; validation, P.H.M.B., K.G., F.G. and S.C.; writing—original draft preparation, M.C., P.H.M.B., K.G. and S.C.; writing—review and editing, P.H.M.B., K.G., F.G., R.B. and S.C.; supervision, R.B. and S.C.; funding acquisition, R.B. and S.C..

Conflicts of interest

"There are no conflicts to declare".

Acknowledgements

The authors thank the French National Research Agency in the framework of the "Investissement d'avenir" program Glyco@Alps (ANR-15-IDEX-02) for PhD and tickets fundings, ANR-18-CE09-0022 and CBH-EUR-GS (ANR-17-EURE-0003). The NanoBio ICMG (UAR 2607), is acknowledged for providing facilities for characterization of block copolymers and glyconanoparticles morphology and size and for SCM images. This work was also supported by the Institute Carnot PolyNat (CARN 0007-01). Arielle Lepellec and Yannig Nedellec are thanked for their daily help in the laboratory.

References

[1] N. Mano, L. Edembe, Bilirubin oxidases in bioelectrochemistry: Features and recent findings, Biosens Bioelectron. 50 (2013) 478–485. https://doi.org/10.1016/j.bios.2013.07.014.

[2] S. Tsujimura, M. Fujita, H. Tatsumi, K. Kano, T. Ikeda, Bioelectrocatalysis-based dihydrogen/dioxygen fuel cell operating at physiological pH, Physical Chemistry Chemical Physics. 3 (2001) 1331–1335. https://doi.org/10.1039/b009539g.

[3] N. Mano, A. de Poulpiquet, O2 Reduction in Enzymatic Biofuel Cells, Chem Rev. 118 (2018) 2392–2468. https://doi.org/10.1021/acs.chemrev.7b00220.

[4] T. Sakurai, K. Kataoka, Basic and applied features of multicopper oxidases, cueo, bilirubin oxidase, and laccase, Chemical Record. 7 (2007) 220–229. https://doi.org/10.1002/tcr.20125.

[5] R. Antiochia, D. Oyarzun, J. Sánchez, F. Tasca, Comparison of direct and mediated electron transfer for bilirubin oxidase from myrothecium verrucaria. Effects of inhibitors and temperature on the oxygen reduction reaction, Catalysts. 9 (2019). https://doi.org/10.3390/catal9121056.

[6] K. Kano, T. Ikeda, Fundamentals and Practices of Mediated Bioelectrocatalysis, 2000. https://doi.org/https://doi.org/10.2116/analsci.16.1013.

[7] K. Kano, Fundamental insight into redox enzyme-based bioelectrocatalysis, Biosci Biotechnol Biochem. 86 (2022) 141–156. https://doi.org/10.1093/bbb/zbab197.

[8] X. Xiao, H.Q. Xia, R. Wu, L. Bai, L. Yan, E. Magner, S. Cosnier, E. Lojou, Z. Zhu, A. Liu, Tackling the Challenges of Enzymatic (Bio)Fuel Cells, Chem Rev. 119 (2019) 9509–9558. https://doi.org/10.1021/acs.chemrev.9b00115.

[9] A. Berezovska, Y. Nedellec, F. Giroud, A.J. Gross, S. Cosnier, Freestanding biopellet electrodes based on carbon nanotubes and protein compression for direct and mediated bioelectrocatalysis, Electrochem Commun. 122 (2021). https://doi.org/10.1016/j.elecom.2020.106895.

[10] I. Mazurenko, A. de Poulpiquet, E. Lojou, Recent developments in high surface area bioelectrodes for enzymatic fuel cells, Curr Opin Electrochem. 5 (2017) 74–84. https://doi.org/10.1016/j.coelec.2017.07.001.

[11] S. Tsujimura, H. Tatsumi, J. Ogawa, S. Shimizu, K. Kano, T. Ikeda, Bioelectrocatalytic reduction of dioxygen to water at neutral pH using bilirubin oxidase as an enzyme and 2,2′-azinobis (3-ethylbenzothiazolin-6-sulfonate) as an electron transfer mediator, Journal of Electroanalytical Chemistry. 496 (2001) 69–75. https://doi.org/https://doi.org/10.1016/S0022-0728(00)00239-4.

[12] S. Tsujimura, From fundamentals to applications of bioelectrocatalysis: Bioelectrocatalytic reactions of FAD-dependent glucose dehydrogenase and bilirubin oxidase, Biosci Biotechnol Biochem. 83 (2019) 39–48. https://doi.org/10.1080/09168451.2018.1527209.

[13] M. Holzinger, A. le Goff, S. Cosnier, Carbon nanotube/enzyme biofuel cells, in: Electrochim Acta, 2012: pp. 179–190. https://doi.org/10.1016/j.electacta.2011.12.135.

[14] H. Shin, S. Cho, A. Heller, C. Kang, Stabilization of a Bilirubin Oxidase-Wiring Redox Polymer by Quaternization and Characteristics of the Resulting O[sub 2] Cathode, J Electrochem Soc. 156 (2009) F87. https://doi.org/10.1149/1.3098481.

[15] A.J. Gross, X. Chen, F. Giroud, C. Travelet, R. Borsali, S. Cosnier, Redox-Active Glyconanoparticles as Electron Shuttles for Mediated Electron Transfer with Bilirubin Oxidase in Solution, J Am Chem Soc. 139 (2017) 16076–16079. https://doi.org/10.1021/jacs.7b09442.

[16] J.L. Hammond, A.J. Gross, F. Giroud, C. Travelet, R. Borsali, S. Cosnier, Solubilized Enzymatic Fuel Cell (SEFC) for Quasi-Continuous Operation Exploiting Carbohydrate Block Copolymer Glyconanoparticle Mediators, ACS Energy Lett. 4 (2019) 142–148. https://doi.org/10.1021/acsenergylett.8b01972.

[17] Y. Suzuki, A. Itoh, K. Kataoka, S. Yamashita, K. Kano, K. Sowa, Y. Kitazumi, O. Shirai, Effects of N-linked glycans of bilirubin oxidase on direct electron transfer-type bioelectrocatalysis, Bioelectrochemistry. 146 (2022). https://doi.org/10.1016/j.bioelechem.2022.108141.

[18] H.Q. Xia, Y. Kitazumi, O. Shirai, K. Kano, Enhanced direct electron transfer-type bioelectrocatalysis of bilirubin oxidase on negatively charged aromatic compound-modified carbon electrode, Journal of Electroanalytical Chemistry. 763 (2016) 104–109. https://doi.org/10.1016/j.jelechem.2015.12.043.

[19] N. Lalaoui, A. le Goff, M. Holzinger, S. Cosnier, Fully Oriented Bilirubin Oxidase on Porphyrin-Functionalized Carbon Nanotube Electrodes for Electrocatalytic Oxygen Reduction, Chemistry - A European Journal. 21 (2015) 16868–16873. https://doi.org/10.1002/chem.201502377.

[20] A. Korani, A. Salimi, Fabrication of High performance bioanode based on fruitful association of dendrimer and carbon nanotube used for design O2/glucose membrane-less biofuel cell with improved bilirubine oxidase biocathode, Biosens Bioelectron. 50 (2013) 186–193. https://doi.org/10.1016/j.bios.2013.05.047.

[21] R.J. Lopez, S. Babanova, Y. Ulyanova, S. Singhal, P. Atanassov, Improved interfacial electron transfer in modified bilirubin oxidase biocathodes, ChemElectroChem. 1 (2014). https://doi.org/10.1002/celc.201300085.

[22] K. So, S. Kawai, Y. Hamano, Y. Kitazumi, O. Shirai, M. Hibi, J. Ogawa, K. Kano, Improvement of a direct electron transfer-type fructose/dioxygen biofuel cell with a substrate-modified biocathode, Physical Chemistry Chemical Physics. 16 (2014) 4823–4829. https://doi.org/10.1039/c3cp54888k.

[23] Y. Ulyanova, S. Babanova, E. Pinchon, I. Matanovic, S. Singhal, P. Atanassov, Effect of enzymatic orientation through the use of syringaldazine molecules on multiple multi-copper oxidase enzymes, Physical Chemistry Chemical Physics. 16 (2014) 13367–13375. https://doi.org/10.1039/c4cp01296h.

[24] F. Giroud, K. Sawada, M. Taya, S. Cosnier, 5,5-Dithiobis(2-nitrobenzoic acid) pyrene derivative-carbon nanotube electrodes for NADH electrooxidation and oriented immobilization of multicopper oxidases for the development of glucose/O2 biofuel cells, Biosens Bioelectron. 87 (2017) 957–963. https://doi.org/10.1016/j.bios.2016.09.054.

[25] N. Lalaoui, K. Gentil, I. Ghandari, S. Cosnier, F. Giroud, Nitrobenzoic acid-functionalized gold nanoparticles: DET promoter of multicopper oxidases and electrocatalyst for NAD-dependent glucose dehydrogenase, Electrochim Acta. 408 (2022). https://doi.org/10.1016/j.electacta.2022.139894.

[26] M. Tominaga, M. Ohtani, I. Taniguchi, Gold single-crystal electrode surface modified with self-assembled monolayers for electron tunneling with bilirubin oxidase, Physical Chemistry Chemical Physics. 10 (2008) 6928–6934. https://doi.org/10.1039/b809737b.

[27] A.J. Gross, R. Haddad, C. Travelet, E. Reynaud, P. Audebert, R. Borsali, S. Cosnier, Redox-Active Carbohydrate-Coated Nanoparticles: Self-Assembly of a Cyclodextrin-Polystyrene Glycopolymer with Tetrazine-Naphthalimide, Langmuir. 32 (2016) 11939–11945. https://doi.org/10.1021/acs.langmuir.6b03512.

[28] P.H.M. Buzzetti, M. Carrière, M. Brachi, K. Gorgy, M. Mumtaz, R. Borsali, S. Cosnier, Organic β-cyclodextrin Nanoparticle: An Efficient Building Block Between Functionalized Poly(pyrrole) Electrodes and Enzymes, Small. 18 (2022). https://doi.org/10.1002/smll.202105880.

[29] M. Brachi, P.H.M. Buzzetti, K. Gorgy, D. Shan, P. Audebert, A. le Goff, H. Li, R. Borsali, S. Cosnier, Trialkoxyheptazine-Based Glyconanoparticles for Fluorescence in Aqueous Solutions and on Surfaces via Controlled Binding in Space, ACS Macro Lett. 11 (2022) 135–139. https://doi.org/10.1021/acsmacrolett.1c00693.

[30] M. Carrière, P. Buzzetti, K. Gorgy, M. Mumtaz, C. Travelet, R. Borsali, S. Cosnier, Functionalizable Glyconanoparticles for a Versatile Redox Platform, Nanomaterials. 11 (2021) 1162. https://doi.org/10.3390/nano11051162.

[31] K. Fukuda, H. Nakahara, T. Kato, Monolayers and Multilayers of Anthraquinone Derivatives Containing Long Alkyl Chains, (1976) 430–438. https://doi.org/https://doi.org/10.1016/0021-9797(76)90323-4.

[32] R.J. Forster, Coupled Proton and Electron Transfer: Adsorbed Anthraquinone-2-carboxylic Acid Monolayers, J Electrochem Soc. 144 (1997) 1165.